The potential role of amyloid β in the pathogenesis of age-related macular degeneration

Takeshi Yoshida,[1] Kyoko Ohno-Matsui,[1] Shizuko Ichinose,[2] Tetsuji Sato,[3] Nobuhisa Iwata,[4] Takaomi C. Saido,[4] Toshio Hisatomi,[5] Manabu Mochizuki,[1] and Ikuo Morita[6]

[1]Department of Ophthalmology and Visual Science and [2]Instrumental Analysis Research Center, Tokyo Medical and Dental University, Tokyo, Japan. [3]Department of Anatomy, School of Dental Medicine, Tsurumi University, Yokohama, Japan. [4]Laboratory for Proteolytic Neuroscience, Institute of Physical and Chemical Research (RIKEN) Brain Science Institute, Wako-shi, Japan. [5]Department of Ophthalmology, Kyushu University, Higashi-ku, Japan. [6]Section of Cellular Physiological Chemistry, Tokyo Medical and Dental University, Tokyo, Japan.

Drusen are extracellular deposits that lie beneath the retinal pigment epithelium (RPE) and are the earliest signs of age-related macular degeneration (AMD). Recent proteome analysis demonstrated that amyloid β (Aβ) deposition was specific to drusen from eyes with AMD. To work toward a molecular understanding of the development of AMD from drusen, we investigated the effect of Aβ on cultured human RPE cells as well as ocular findings in *neprilysin* gene–disrupted mice, which leads to an increased deposition Aβ. The results showed that Aβ treatment induced a marked increase in VEGF as well as a marked decrease in pigment epithelium-derived factor (PEDF). Conditioned media from Aβ-exposed RPE cells caused a dramatic increase in tubular formation by human umbilical vein endothelial cells. Light microscopy of senescent neprilysin gene–disrupted mice showed an increased number of degenerated RPE cells with vacuoles. Electron microscopy revealed basal laminar and linear deposits beneath the RPE layer, but we did not observe choroidal neovascularization (CNV). The present study demonstrates that Aβ accumulation affects the balance between VEGF and PEDF in the RPE, and an accumulation of Aβ reproduces features characteristic of human AMD, such as RPE atrophy and basal deposit formation. Some other factors, such as breakdown of integrity of Bruch membrane, might be necessary to induce CNV of AMD.

Introduction

Amyloid β (Aβ) peptides vary in length from 39 to 43 amino acid residues and are produced by the sequential proteolytic processing of amyloid precursor protein (APP) by the β site APP cleaving enzyme (1) and a presenilin complex (2). Increased evidence suggests that the conversion of Aβ from monomeric form to oligomeric or aggregated form in the brain is a key event in the pathogenesis of Alzheimer disease (AD). Aβ is known to be a physiological peptide, the steady state level of which is maintained by a metabolic balance between synthesis and degradation (3–6), and is constitutively secreted from cells (4, 7). Under physiological conditions, Aβ is degraded by peptidases, such as neprilysin, immediately after production (5, 6). Numerous studies have shown that Aβ peptide deposition in the brain stimulates microglia and contributes to neuronal apoptosis (8–11).

New evidence indicates that, in age-related macular degeneration (AMD), substructural elements within drusen contain Aβ (12–14), which is a major component of senile plaques and cerebrovascular deposits in the brains of patients with AD. Dentchev et al. demonstrated that Aβ deposition is specific to drusen from eyes of patients with AMD; 4 of 9 AMD retinas and 0 of 9 normal retinas had Aβ-positive drusen (13). Anderson et al. (14) demonstrated that Aβ assemblies are most prevalent in eyes with moderate or high drusen loads and suggested that Aβ might be associated with the more advanced stages of AMD. AMD is the leading cause of irreversible vision loss among the elderly in developed countries (15–18). Vision may be impaired as a consequence of geographical atrophy (dry or nonexudative AMD) or choroidal neovascularization (CNV) (wet or exudative AMD). Many studies have confirmed that the presence of the drusen, identified as gray-yellow deposits that build up in or around the macula of the retina, represents a significant risk factor for the development of visual loss from AMD (19–21). Drusen are deposited and located just beneath the retinal pigment epithelial (RPE) cell layer (22). It is believed that they may signal the presence of an altered pathophysiology of the RPE and, consequently, they may be a marker for the degree of diffuse RPE dysfunction in patients with AMD (23). However, it still remains unclear which component of drusen is a key contributor to the progression of AMD.

The RPE is a monolayer of highly specialized cells located between the neural retina and the vascular choroid that influences the structure and function of cells in both (24, 25). Among various growth factors secreted from RPE cells, it appears that VEGF plays a central role in the progression of CNV secondary to AMD. In patients with AMD, high concentrations of VEGF and VEGF receptors have been detected in the subfoveal fibrovascular membrane, the surrounding tissue, and the RPE (26, 27). Recent studies, however, question the importance of VEGF alone in promoting CNV because, in transgenic mice overexpressing

Nonstandard abbreviations used: Aβ, amyloid β; AD, Alzheimer disease; AMD, age-related macular degeneration; APP, amyloid precursor protein; CNV, choroidal neovascularization; CRALBP, cellular retinaldehyde-binding protein; DAB, diaminobenzidine-tetrahydrochloride; HUVEC, human umbilical vein endothelial cell; PEDF, pigment epithelium-derived factor; RPE, retinal pigment epithelium; TSA, tyramide signal amplification.

Conflict of interest: The authors have declared that no conflict of interest exists.

Citation for this article: *J. Clin. Invest.* **115**:2793–2800 (2005). doi:10.1172/JCI24635.

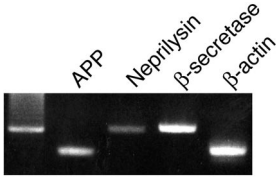

Figure 1
RT-PCR detection of APP, neprilysin, and β-secretase in human RPE cells. Human RPE cells were cultured in DMEM containing 10% FCS. After cellular confluence, total RNA was extracted from cultured RPE cells. The cDNA was synthesized from 2 μg of total RNA, and the reaction product was subjected to PCR amplification using specific primers for APP, neprilysin, and β-secretase.

VEGF in photoreceptors (28) and the RPE (29), CNV penetrating through the Bruch membrane was not found.

Angiogenesis is thought to result from an imbalance between angiogenic factors and antiangiogenic factors (30, 31). A potent antiangiogenic factor was recently identified in the retina and shown to be secreted by RPE cells (32–34). This factor, pigment epithelium-derived factor (PEDF), was shown to be a very potent inhibitor of neovascularization in a murine model of ischemia-induced retinopathy (35). However, the reason for the imbalance between VEGF and PEDF is not known.

In the present study, we hypothesized that Aβ accumulated in drusen might induce the change of the expression of angiogenesis-related factors and cause cellular dysfunction in the RPE and therefore play a key role in the development of AMD. To work toward a molecular understanding of the development of AMD from drusen, we investigated the effect of Aβ on cultured human RPE cells as well as ocular findings in *neprilysin* gene–disrupted mice, which leads to an increased deposition of Aβ. The results demonstrated that Aβ has the potential to promote angiogenesis by modulating the expression of angiogenesis-related factors released from RPE cells in vitro. In addition, the increased deposition of Aβ in genetically modified mice reproduced many of the features of human AMD, including subretinal formation of basal deposits and RPE degeneration. These results suggest that Aβ may be a key contributor to the development of AMD.

Results

Expression of APP, neprilysin, β-secretase mRNA, and protein in RPE in vitro and in vivo. RT-PCR analysis identified the expression of mRNA for APP, β-secretase, and neprilysin in human RPE cells (Figure 1). Also, intense immunoreactivity for APP, neprilysin, and β-secretase protein was detected in the RPE cell layer of ddY mice by diaminobenzidine-tetrahydrochloride (DAB) staining (Figure 2). These results indicate the possibility that human RPE cells mediate and modulate the expression of Aβ.

Modulation of VEGF and PEDF gene expression by Aβ in RPE cells. We next investigated how Aβ modulates the expression of angiogenesis-related factors in RPE cells. We examined expression of 2 representative angiogenesis-related factors: VEGF, a potent angiogenic factor; and PEDF, a novel antiangiogenic factor. According to the results of real-time PCR, VEGF mRNA levels in RPE cells treated with $A\beta_{1-40}$ for 24 hours were 2.5 ± 0.15 times higher than those in untreated cells ($P < 0.01$). Also, $A\beta_{1-40}$ increased the secretion of VEGF protein as measured by ELISA (Figure 3). Although PEDF mRNA expression was not changed after treatment with $A\beta_{1-40}$ (PEDF mRNA levels in RPE cells treated with Aβ were 0.948 ± 0.055 times those in untreated cells), Western blot analysis revealed that it decreased PEDF protein expression to 0.46 ± 0.12 times that in untreated RPE cells ($P < 0.01$). In addition, the expression of mRNA for cellular retinaldehyde–binding protein (CRALBP), a differentiation-specific gene in RPE cells, was significantly decreased when the RPE cells were exposed to $A\beta_{1-40}$. The expression of CRALBP mRNA in cells treated by Aβ was 0.48 ± 0.01 times that in untreated cells ($P < 0.01$). These effects were not mimicked with the reverse control $A\beta_{40-1}$. The mRNA levels of cells treated with control $A\beta_{40-1}$ were 1.03 ± 0.02 (for VEGF), 0.91 ± 0.07 (for PEDF), 0.90 ± 0.02 (for CRALBP) times those in untreated cells. Also, PEDF protein levels of $A\beta_{40-1}$–treated cells were 1.05 ± 0.09 times that in untreated cells per Western blotting.

Angiogenic activity of conditioned media from Aβ-treated RPE cells. RPE cells were treated with or without 25 μM $A\beta_{1-40}$, and the angiogenic activity of their conditioned media was assessed with an angiogenesis assay kit (Kurabo). There was a marked increase in tube-like structures when the human umbilical vein endothelial cells (HUVECs) were cultured in the presence of conditioned media from $A\beta_{1-40}$–treated RPE cells compared with conditioned media from RPE cells not receiving Aβ or conditioned media from $A\beta_{40-1}$–treated RPE cells (Figure 4, A–C). Addition of 25 μM $A\beta_{1-40}$ alone to HUVECs did not promote tube formation (Figure 4D). Quantitative analysis of total tube length confirmed that there was a significant increase in tube formation when HUVECs were incubated with conditioned media from $A\beta_{1-40}$–treated cells compared with when they were treated with conditioned media from cells not receiving Aβ or with conditioned media from cells treated with $A\beta_{40-1}$ (Figure 4E).

Light microscopic findings of senescent neprilysin gene–disrupted mice. Eyes from senescent neprilysin-deficient and age-matched wild-type mice (27 months) were histopathologically examined. Light microscopy of H&E-stained paraffin sections from 27-month-old senescent neprilysin gene–disrupted mice showed an increased number of degenerated cells with vacuoles in the RPE (Figure 5,

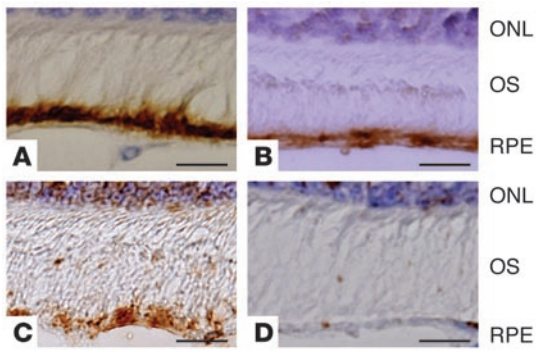

Figure 2
Immunohistochemical detection of APP, neprilysin, and β-secretase in the RPE cell layer of albino ddY mice. Paraformaldehyde-fixed sections from eyeballs of male albino ddY mice were stained for APP (**A**), neprilysin (**B**), or β-secretase (**C**). Immune complexes were detected with DAB as a brown reaction product. Immunoreactivity for APP, neprilysin, and β-secretase was observed in the RPE cell layer. DAB staining was absent when nonimmune serum was substituted for the primary antibody (**D**). Scale bars: 20 μm (**A**–**D**). ONL, outer nuclear layer; OS, outer segment.

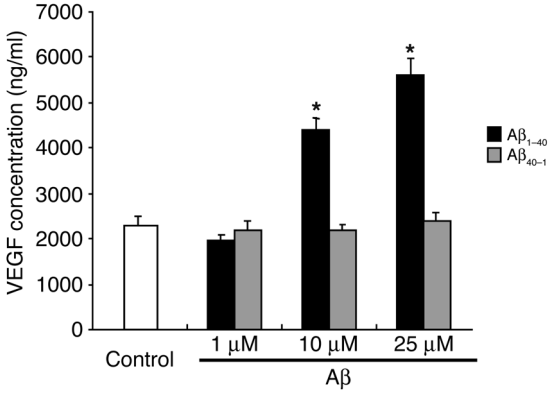

Figure 3
Concentration of immunoreactive VEGF in culture supernatants of RPE cells. Human RPE cells were incubated with various concentrations of Aβ (1–25 μM), and VEGF protein expression in the culture supernatants was analyzed by ELISA after 24 hours of culture. Values are expressed as mean ± SEM. $n = 3$; $^*P < 0.05$.

B and D). In contrast, no such changes were visible in wild-type mice (Figure 5, A and C). The photoreceptor layer appeared normal in both types of mice.

Upregulation of VEGF and downregulation of PEDF in neprilysin gene–disrupted mice. We further investigated the expression of VEGF and PEDF in both neprilysin gene–disrupted mice and wild-type mice. Immunohistochemical analysis demonstrated that in senescent neprilysin gene–disrupted mice, VEGF production was upregulated and PEDF production was downregulated in the RPE cell layer compared with age-matched wild-type mice (Figure 6). However, new vessel formation was not observed in neprilysin gene–disrupted mice even when they were examined by immunostaining for vWF (data not shown).

Electron microscopic findings of senescent neprilysin gene–disrupted mice. Electron microscopy revealed that the RPE cells in neprilysin gene–disrupted mice showed an increase in the number of cytoplasmic vacuoles (Figure 7A), as shown by light microscopic examination (Figure 5, B and D). Transmission electron microscopy sections revealed that the RPE cells had lost their defined tight and adherens junctions and that intercellular space developed between some of the adjacent cells (Figure 7B). The most striking feature from neprilysin gene–disrupted mouse retinas was the presence of extensive deposits, which were mainly situated between the plasma membrane and the basal lamina of RPE cells (Figure 7, A–C), although some were located between the basal lamina of RPE cells and the inner collagenous layer of the Bruch membrane (Figure 7C). Based on their morphological characteristics, the former appear to be the basal laminar deposits and the latter the basal linear deposits. These regions contained substantial subepithelial deposits whereas the basal infoldings of the RPE cells were often distorted and the space between them enlarged. Photoreceptor outer segments were accumulated in the subretinal space, which suggests dysfunction of RPE cells (Figure 7A). In contrast, these findings, like subepithelial deposit formation and cytoplasmic vacuoles within RPE cells, were not observed in age-matched wild-type mice retinas (Figure 7, D–F). Immunoelectron microscopy revealed that subepithelial deposits were stained by anti-Aβ antibody (Figure 8). Aβ staining was also detected within RPE cells overlying subepithelial deposits (Figure 8E). However, there was no migration or proliferation of choroidal endothelial cells or fibroblasts that would indicate the development of CNV.

Figure 4
Effects of the conditioned media from RPE on in vitro angiogenesis. HUVECs cocultured with fibroblasts were incubated with a 1:1 mixture of the supernatant of RPE cells and endothelial cell culture media. After 10 days of culture, the cells were fixed and stained with vWF. Representative phase-contrast microscopic images are shown (**A**–**D**). The supernatant used was conditioned by RPE cells without exposure to Aβ (**B**) or with exposure to 25 μM $Aβ_{40–1}$ (**C**) or 25 μM $Aβ_{1–40}$ (**D**) for 24 hours. In **A**, 25 μM $Aβ_{1–40}$ alone was mixed with the endothelial cell culture media. (**E**) The total length of tube-like structures in HUVECs. The area of capillary growth was quantitated with an image analyzer in 8 different fields for each condition at ×10 magnification and statistically analyzed. Data are expressed as mean ± SEM. Asterisk indicates that the value is significantly greater than that of the corresponding control. $n = 3$; $P < 0.01$.

Discussion

AMD is the principal cause of irreversible blindness in patients over the age of 60 in developed countries (15–18). The earliest clinically visible abnormality in AMD is drusen, which are the extracellular deposits accumulated between the RPE and the Bruch membrane. However, it still remains unclear which component of drusen is a key contributor to the progression of AMD. Recent studies (12–14) have shown that age-related ocular drusen contain Aβ, which has been implicated as a central factor in the pathogenesis of AD (36). Aβ is a physiological peptide in the brain, and its steady state levels are determined by the balance between its synthesis and degradation (3–6). Neprilysin (EC 3.4.24.11) is a membrane-bound zinc metallopeptidase that has a rate-limiting role in Aβ catabolism (5, 37). Iwata et al. (6) demonstrated that downregulation of neprilysin is likely to be related to AD pathology.

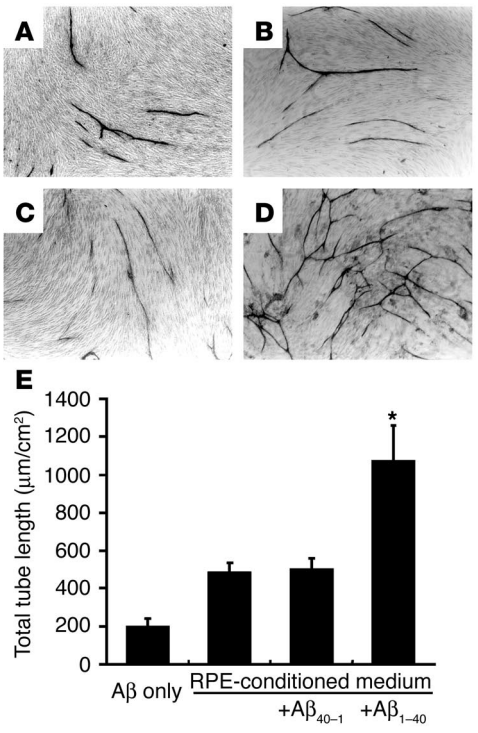

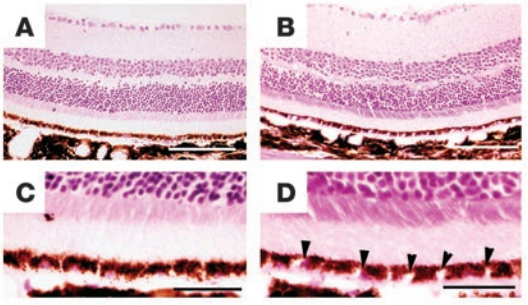

Figure 5
Light microscopy of H&E-stained sections of 27-month-old neprilysin-deficient (**B** and **D**) and age-matched wild-type (**A** and **C**) mice retinas. **C** and **D** show magnified views of **A** and **B**, respectively. (**A** and **C**) Morphology of normal retina from age-matched wild-type mice. (**B** and **D**) Morphology of senescent neprilysin-deficient mice showing degenerated cells with vacuoles in the RPE layer (arrowheads). Scale bars: 150 μm (**A** and **B**); 30 μm (**C** and **D**).

In the present study, we focused on Aβ among the various components of drusen and investigated the effect of Aβ on cultured human RPE cells as well as ocular findings in mice lacking the neprilysin gene. The expression of APP and β-secretase was detected in human RPE as well as in the RPE layer of mouse eyes, as described previously (12, 38). In addition, we have demonstrated the expression of neprilysin in RPE. These results point strongly toward an RPE origin for Aβ peptides.

Although what causes the alteration in the Aβ metabolism of RPE is unknown, Frederikse et al. (39) demonstrated that APP and Aβ are present at low levels in normal lenses and increase in intact cultured monkey lenses treated with H_2O_2 or UV radiation. Because oxidative stress is considered an important stimulus for the development of AMD (31, 40), it might affect Aβ metabolism in RPE cells, which could eventually lead to Aβ deposition in aging human retina.

We further demonstrated that Aβ upregulated VEGF gene expression in both mRNA and protein levels, but decreased PEDF only in protein levels in human RPE cells. This indicates that the regulation of PEDF expression by Aβ may be at a posttranscriptional level, as shown by Dawson et al. (34). In addition, conditioned media from Aβ-treated RPE cells dramatically increased tubular formation by HUVECs, suggesting that Aβ has the potential to induce CNV in vivo. Aβ treatment also downregulated the expression of CRALBP, which is a known marker for differentiation of RPE cells (41). Human CRALBP gene defects can either tighten or abolish retinoid interactions, which in turn can compromise substrate carrier interactions with 11-*cis*-retinol dehydrogenase and lead to several retinal pathologies (42). These results combined with the previous data suggest that accumulation of Aβ acts on RPE cells, which affects the gene expression profile of RPE cells and causes dysfunction of RPE.

In senescent neprilysin-deficient mice, an animal model for AD, we showed Aβ accumulation between RPE and the Bruch membrane in the eye as well as enhanced VEGF expression and diminished PEDF expression in the RPE layer, suggesting an imbalance between the expression of angiogenesis-related factors. Additionally, the neprilysin gene–disrupted mice express traits that resemble those present in AMD, such as degenerative changes of RPE cells and accumulation of sub-RPE deposits. Subepithelial deposits are classified into 2 distinct types ultrastructurally, a basal laminar deposit and a basal linear deposit (22), and both have been strongly associated with AMD (22, 43). This indicates that neprilysin gene–disrupted mice can be used as animal models to study early stages of AMD as well as the progression to an advanced form.

It is well known that Aβ induces apoptotic cell death in cultured neurons (44). Dentchev et al. (13) reported that the highest quantity of Aβ-containing vesicles occurred near the edges of atrophy in human eyes with geographic atrophy (an advanced form of AMD), and they suggested that Aβ may contribute to the pathogenesis of RPE degeneration. Although the mechanism through which Aβ deposition causes RPE degeneration and dysfunction in neprilysin gene–disrupted mice is unclear, previous studies have suggested a central role for oxidative stress as a cause of Aβ-induced neuronal cell death (45, 46). Oxidative stress has been reported to cause upregulation of VEGF (47) and downregulation of PEDF (31) in human RPE cells. It has also been demonstrated that oxidative stress induces RPE cell death (48) and downregulation of differentiation-specific genes such as CRALBP in human RPE cells (49) and that it could be responsible for retinal ultrastructural alterations (50). Recent studies have also suggested that Aβ-induced cell death could arise from dysfunction of the ER (51). ER stress might be implicated in RPE degeneration seen in senescent neprilysin gene-deficient mice.

However, new vessel formation, another hallmark of exudative AMD, was not obvious in senescent neprilysin gene–disrupted mice histologically. Also, fundus angiography using fluorescein and indocyanine green dye did not reveal dye leakage, suggesting no CNV (data not shown). Although some studies have demonstrated that a breakdown of the critical balance between VEGF and PEDF is a key contributor to the development of CNV in AMD (31, 52), an imbalance between VEGF and PEDF in RPE in these knockout mice did not result in subsequent CNV formation penetrating the Bruch membrane, as seen in human AMD. These conflicting results from the cell culture system and animal models are difficult to explain. One possibility is that the structural components of the Bruch membrane must be compromised for CNV to occur. This possibility is supported by Schwesinger et al. (29) who reported that, in transgenic mice that overexpress VEGF in the RPE, an intact Bruch membrane prevents CNV from penetrating into the subretinal space. Clinical disorders with breaks in the Bruch membrane,

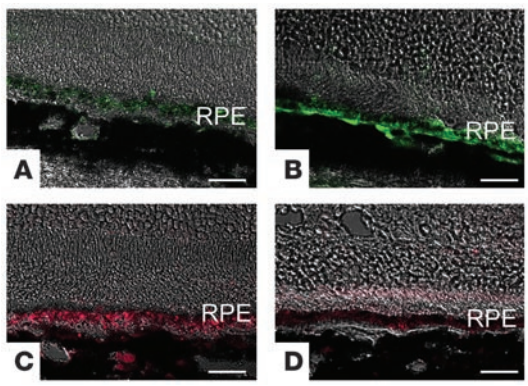

Figure 6
Fluorescent micrographs of paraformaldehyde-fixed sections from 27-month-old neprilysin-deficient (**B** and **D**) and age-matched wild-type mouse (**A** and **C**) retinas. The sections were treated with antibodies against VEGF (FITC: **A** and **B**) or antibodies against PEDF (Texas Red: **C** and **D**). Scale bars: 40 μm (**A**–**D**).

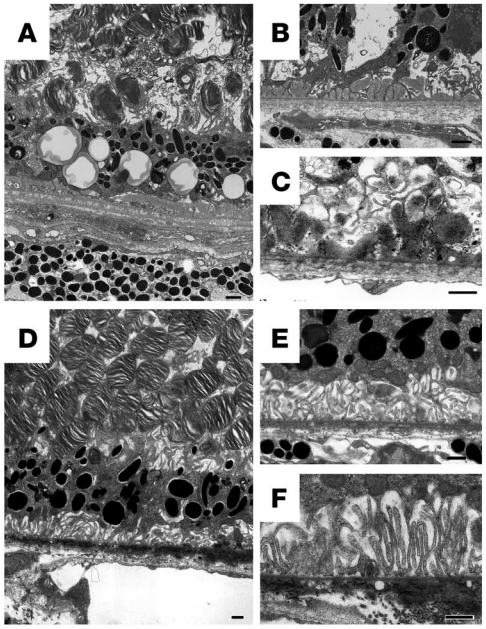

Figure 7
Electron micrographs of retinas from a 27-month-old neprilysin gene–disrupted mouse (**A**–**C**) and an age-matched wild-type mouse (**D**–**F**). (**A**) An RPE cell layer from the retina of a senescent neprilysin gene–disrupted mouse. Note the abundant cytoplasmic vacuoles among attenuated RPE cells. (**B**) Disruption of junction structures between RPE cells and substantial subepithelial deposits. (**C**) An electron micrograph of extensive deposits beneath RPE cells. (**D**) An RPE cell layer from the retina of a senescent wild-type mouse. RPE cell layer shows normal appearance. Cytoplasmic vacuoles among RPE cells are not obvious. (**E** and **F**) Basal infoldings of RPE cells are prominent, and no subepithelial deposits are observed. Scale bars: 1 μm (**A**–**F**).

such as pathologic myopia, trauma, pseudoxanthoma elasticum, and histoplasmosis, show an increased incidence of CNV. Furthermore, recent study has suggested that the integrity and thickness of the macular elastic layer of the Bruch membrane in patients with CNV related to AMD were significantly lower as compared with that in unaffected and age-matched controls (53). The second possibility is that the 27-month-old mice are not senescent enough to mimic aged human subjects. These findings suggest that further aging or loss of the integrity of the Bruch membrane in addition to Aβ deposition might be necessary to induce CNV that penetrates into the subretinal space. The remaining possibility is the regulation of the complement activation system. It was demonstrated that Aβ colocalizes with activated complement components in amyloid vesicles within drusen (12), and Aβ is considered to play a primary role in the activation of complement-mediated events during drusen formation. Very recently, 3 different groups showed that a variant in the complement factor H (CFH) gene was strongly associated with AMD (54–56). The CFH gene is a key regulator of the complement system of innate immunity (57) and inhibits the activation of C3 to C3a and C3b. Taken together, the dysregulation of complement activation system and Aβ deposition might facilitate the development of CNV. This should be investigated in the future.

Figure 8
Localization of Aβ in sub-RPE deposits from neprilysin gene–disrupted mice by indirect immunogold labeling. Cryostat sections were prepared from senescent neprilysin gene–disrupted mice and incubated with anti-Aβ antibody (4G8) and anti-mouse 10- to 15-nm gold conjugate (for scanning electron microscopy images) or 5- to 10-nm gold conjugate (for transmission electron microscopy images). Gold particles were present within the subretinal deposit (**C** and **E**) as well as in the cytoplasm of RPE cells (**E**, arrowheads). **A**–**C** are scanning electron microscopy images. **B** shows higher magnification of **A**, and **C** shows higher magnification of **B**. **D** and **E** are transmission electron microscopy images. **E** shows higher magnification of **D**. DE, subretinal deposit; BM, Bruch membrane; CH, choroid. Scale bars: 10 μm (**A**); 3.6 μm (**B**); 360 nm (**C**); 1 μm (**D**); and 0.1 μm (**E**).

The results in the present study could also indicate a common pathogenic mechanism between AMD and AD as an age-related pathology. Recently, a link has also been suggested between supranuclear cataracts and AD (58–60). These studies suggested that amyloid fibrils might be associated with pathological symptoms in a diverse age-related illness, although their specific role in inducing disease might differ depending on the tissue. Currently, various therapeutic approaches for clearing Aβ plaques are being tested as treatments for AD, including vaccination against Aβ (61), topical application of an anti-Aβ antibody (62), and adeno-associated viral vector–mediated gene transfer of neprilysin (63). Some of these might be effective against the development of AMD from drusen. Thus, further investigation of the role of Aβ in AMD pathogenesis is warranted.

Methods

Materials. DMEM and TRIzol reagent were from Invitrogen Corp.; plasticware (Falcon) was from BD; fetal calf serum was from HyClone; the VEGF ELISA kit and recombinant basic FGF were from BioSource International; laminin was from Upstate; You-Prime First-Strand Beads, PCR beads, and nylon membranes were from Amersham Pharmacia Biotech; agarose was from Takara; $A\beta_{1-40}$ (HCl form) was from Peptide Institute Inc.; fluorescein isothiocyanate–

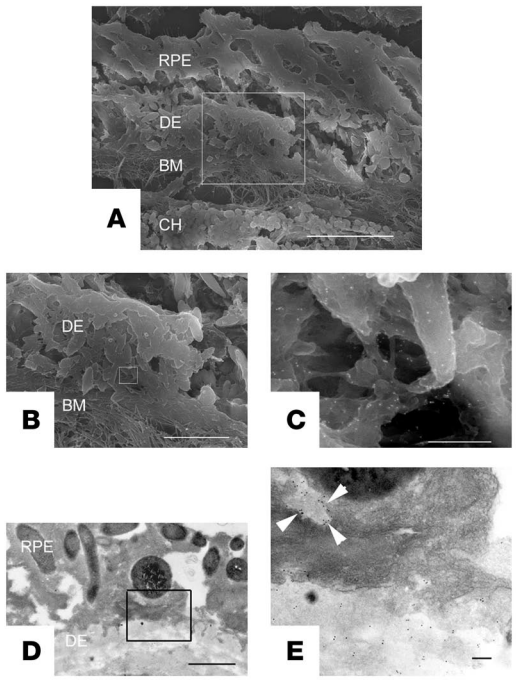

conjugated and Texas Red–conjugated goat antibodies to mouse IgG were from Sigma-Aldrich; and the in vitro angiogenesis kit was from Kurabo.

Human RPE cell culture. Primary cultures of human RPE cells were a generous gift from Peter A. Campochiaro (Wilmer Eye Institute, Johns Hopkins University, Baltimore, Maryland, USA). The cultures used for the experiments described here were in the second to fourth passage at the time of separation. Cultures were demonstrated to be pure populations of RPE cells by immunocytochemical staining for cytokeratins (data not shown). Differentiated RPE cells were established as described previously (30, 39). RPE cell cultures were maintained in DMEM supplemented with 10% FBS and 10 ng/ml basic FGF. The cells exhibited epithelioid morphology and expressed CRALBP, a marker for differentiation of RPE cells (39).

RPE cells were subcultured into 24-well tissue culture plates at a density of 4×10^4 cells. Seven days after reaching confluence, the medium was changed and cells were incubated in serum-free DMEM in the presence or absence of $A\beta_{1-40}$ peptide (HCl form) at a concentration of 1, 10, or 25 μM. After 24 hours, the medium was collected, filter sterilized, and stored at –80°C until use for tube-formation assay, Western blot analyses, and ELISA. The cells were also homogenized and used for RNA extraction. Each condition was examined in triplicate, and results were repeated in at least 3 independent experiments.

Semiquantitative RT-PCR for APP, neprilysin, and β-secretase. Total RNA was extracted from cultured RPE cells using TRIzol reagent. The cDNA was synthesized from 2 μg of total RNA using You-Prime First-Strand Beads according to the manufacturer's protocol, and the reaction product was subjected to PCR amplification using the GeneAmp PCR System (Cetus; PerkinElmer). Human APP, neprilysin, and β-secretase mRNAs were detected using the following primers: for APP (GenBank accession number NM000484), 5′-TCAGATCCGGTCCCAGGTTATG-3′ (forward) and 5′-AGAGTCAGCCCCAAAAGAATGC-3′ (reverse); for neprilysin (58), 5′-GTGCCCAGCAGTCCAACTCATTGAAC-3′ (forward) and 5′-CCCCATTTCTGTGGTGTTGGCAAGTC-3′ (reverse); and for β-secretase (59), 5′-CATTGGAGGTATCGACCACTCGCT-3′ (forward) and 5′- CCACAGTCTTCCATGTCCAAGGTG-3′ (reverse). The PCR reaction for APP was repeated for 25 cycles, and each cycle included denaturation at 94°C for 1 minute, annealing at 60°C for 1 minute, and primer extension at 72°C for 2 minutes. The PCR reaction for neprilysin was repeated for 32 cycles, and each cycle included denaturation at 94°C for 1 minute, annealing at 60°C for 1 minute, and primer extension at 72°C for 2 minutes. The PCR reaction for β-secretase was repeated for 32 cycles, and each cycle included denaturation at 94°C for 1 minute, annealing at 62°C for 1 minute, and primer extension at 70°C for 2 minutes. The expected size of the reaction products was 313 bp for APP, 610 bp for neprilysin, and 624 bp for β-secretase. For the detection of β-actin mRNA, the following primers were used: 5′-CTTCGCGGGCGACGATGC-3′ (forward) and 5′-CGTACATGGCTGGGGTGTTG-3′ (reverse). The expected size of the reaction product was 340 bp for β-actin.

Immunohistochemical analysis of APP, neprilysin, and β-secretase in RPE. For immunohistochemistry of APP, β-secretase, and neprilysin in RPE cells, male albino ddY mice (8 to 10 weeks old) were used. All experiments were approved by the Ethics Committee for Animal Use in Research and Education of the Tokyo Medical and Dental University and conformed to the Association for Research in Vision and Ophthalmology Statement for the Use of Animals in Ophthalmic and Vision Research. The mice were deeply anesthetized with pentobarbital (50 mg/kg) and perfused transcardially with 0.1 M phosphate-buffered saline (PBS: pH 7.4), followed by ice-cold phosphate-buffered 4% paraformaldehyde or 10% neutral-buffered formalin. Eyeballs were removed, immersed in the same fixative for 6 hours at room temperature, and then embedded in paraffin blocks. The antibodies used included mouse monoclonal antibody MAB348 against APP (1:200; Chemicon International), mouse monoclonal antibody NCL-CD10-270 against neprilysin (1:100; Novocastra), and rabbit polyclonal antibody BACE1 against β-secretase (1:200; Molecular Biologische Technologie). We performed immunostaining of APP, neprilysin, and β-secretase using the high-temperature antigen-unmasking technique and the immunoperoxidase-indirect tyramide signal amplification (TSA) method (60). After deparaffinization and rehydration, sections were heated in an autoclave at 121°C for 5 minutes in 10 mM sodium citrate buffer (pH 6.0) for epitope retrieval of antigen, and endogenous peroxidase was then inactivated with 0.3% hydrogen peroxide in methanol. To block nonspecific immunoreactivity, the sections were sequentially treated with the blocking solutions supplied in a biotin/avidin blocking kit (Vector Laboratories) and a TSA kit (TSA Biotin System; PerkinElmer). Antibodies diluted in 0.1 M Tris-HCl, pH 7.5, containing 0.15 M NaCl were reacted overnight at 4°C. After rinsing 3 times in TNT buffer (0.1 M Tris-HCl, 0.15 M NaCl, and 0.05% Tween 20, pH 7.5) for 5 minutes, the sections were sequentially incubated with biotinylated goat anti-mouse or anti-rabbit IgG1 (1:3,000; SouthernBiotech) for 1 hour, with horseradish peroxidase–conjugated streptavidin for 30 minutes (1:100; supplied in the TSA Biotin System), followed by biotinylated tyramide for 10 minutes (1:50 in amplification solution; supplied in the TSA Biotin System) at room temperature. Tyramide-enhanced immunoreactivity was visualized with DAB, and eosin-staining was used for counterstaining.

Light cycler real-time PCR. Total RNA was extracted from cultured RPE cells using TRIzol reagent. The cDNA was synthesized from 2 μg of total RNA using You-Prime First-Strand Beads according to the manufacturer's protocol. The cDNA was subjected to quantitative PCRs on a LightCycler Instrument (Roche Diagnostics Corp.) using QuantiTect SYBR Green PCR Kit (QIAGEN) for VEGF, PEDF, GAPDH, and the discriminative cellular markers, CRALBP. PCR amplifications were performed with specific primers in a total volume of 20 μl containing 2 μl of sense and antisense primer mixture (5 μM of each primer), 10 μl of 2xSYBR Green QPCR Master Mix (QIAGEN), 1 μl of 1:10 diluted cDNA and nuclease-free PCR-grade water. The mixture was used as a template for the amplification after initial denaturation at 95°C and 40–45 cycles (95°C for 30 seconds, 55–58°C for 1 minute, and 72°C for 30 seconds). The primer sequences were as follows: for human VEGF, 5′-ATCGAGTACATCTTCAAGCCAT-3′ (sense) and 5′-CTTTCTTTGGTCTGCATTCACA-3′ (antisense); for human PEDF, 5′-TTACGAAGGCGAATCACCA-3′ (sense) and 5′-TAAGGTGATAGTCCAGCGGG-3′ (antisense); for GAPDH, 5′-ACCACAGTCCATGCCATCAC-3′ (sense) and 5′-TCCACCACCCTGTTGCTGTA-3′ (antisense); and for human CRALBP, 5′-GCTGCTGGAGAATGAGGAAACT-3′ (sense) and 5′-TGAACCGGGCTGGGAAGGAATC-3′ (antisense) (61). SYBR Green fluorescence was measured, and quantification of each PCR product was expressed relative to GAPDH.

ELISA and Western blot analysis. The amount of secreted VEGF in conditioned media from RPE cells was determined using a commercial ELISA kit according to the manufacturer's instructions. The absorbance was measured at 450 nm in a Bio-Rad Model 450 microplate reader (Bio-Rad Laboratories). For standardization, serial dilutions of recombinant VEGF were assayed.

For Western blot analysis of secreted PEDF, cells were maintained in serum-free media for 48 hours before harvest for protein. Final protein concentrations were determined using a BCA assay (Pierce Chemical Co.) according to the manufacturer's instructions. Equal amounts of secreted protein (8 μg) were separated by 12% sodium dodecyl sulfate-polyacrylamide gel electrophoresis and electrophoretically transferred onto nylon membranes. Nylon membranes containing transferred proteins were pre-

treated with 1.0% nonfat dried milk in 50 mM Tris (pH 8.0) and then incubated overnight with a monoclonal antibody against human PEDF. PEDF immunoreactivity was visualized by exposing x-ray film to blots incubated with ECL reagent (Amersham Biosciences).

Tube formation assay by HUVECs. Experiments on tube formation were conducted in triplicate in 24-multiwell dishes using an angiogenesis kit (Kurabo) according to the manufacturer's instructions. Briefly, the conditioned medium from Aβ-treated RPE cells was collected and diluted 1:1 with endothelial cell medium (Kurabo). HUVECs cocultured with human fibroblasts were cultured in the presence of the conditioned medium for 5 days. Media were changed every 2 days. Thereafter, dishes were washed with PBS and then fixed with 70% ethanol at 48°C. After the fixed cells were rinsed twice with PBS, cells were incubated with sheep anti-human vWF in PBS containing 10% FBS for 60 minutes. After washing 5 times with PBS containing 10% FBS, cells were incubated for 60 minutes with donkey anti-sheep IgG conjugated with horseradish peroxidase. Metal-enhanced DAB was used as a substrate, and the reaction yielded a dark reddish-brown insoluble product. Finally, the cells were washed 5 times with PBS and then viewed in an Olympus BHS system microscope (Olympus). Tube length was measured quantitatively with an image analyzer (in mm/cm^2) in 8 different fields for each condition, and the results were subjected to statistical analysis.

Neprilysin gene–disrupted mice and tissue preparation. Senescent neprilysin-deficient and wild-type mice (27 months old) (3, 62) were used for the experiments. Fixed eyeballs were embedded in paraffin blocks. Mounted sections were defatted in xylene and hydrated in a grade series of ethanol in water. For immunohistochemical staining of angiogenesis-related factors, eyes were enucleated, and 8-μm cryostat sections were prepared. Sections were treated with 0.3% H_2O_2 and 20% normal goat serum to block endogenous peroxidase and nonspecific binding, respectively. The sections were then treated overnight at 4°C with rabbit polyclonal antibody against VEGF (1:3,000 dilution; Santa Cruz Biotechnology Inc.) or rabbit polyclonal antibody against PEDF (1:3,000 dilution; Trans Genic Inc.). After directly reacting the sections for 60 minutes at room temperature with fluorescein isothiocyanate– or Texas Red–conjugated goat anti-rabbit antibodies (1:400; Sigma-Aldrich), images were obtained with a Zeiss LSM 510 confocal microscope.

Electron microscopy. Eyeballs were fixed in 2.5% glutaraldehyde in 0.1 M PBS for 2 hours. The eyeballs were washed overnight at 4°C in the same buffer and postfixed for 2 hours with aqueous OsO_4 in 0.1 M PBS. The tissue was dehydrated through a graded ethanol series and embedded in Epon 812 (TAAB Laboratories Equipment Ltd.). Ultrathin (70 nm) sections were collected on copper grids and double-stained with uranyl acetate and lead citrate and then examined with an H-7100 transmission electron microscope (Hitachi Ltd.).

For immunoelectron microscopy of Aβ, 8-μm cryostat sections were used. The sections were placed on silane-coated glass and then placed on droplets of 1% bovine serum albumin in 0.1 M PBS on a parafilm sheet for 1 hour at 4°C to eliminate nonspecific antibody binding. The slides were then placed on droplets of mouse monoclonal antibody against Aβ 4G8 (1:50; Signet Laboratories) containing 1% bovine serum albumin for 48 hours at 4°C. Each slide was washed with 0.1 M PBS and incubated with goat anti-mouse IgG and IgM conjugated with 5- to 10-nm–diameter gold colloidal particles (1:20; British Biocell International). After incubation, the slides were washed with 0.1 M PBS for 2 hours. The sections on the slide were subsequently fixed in 2.5% glutaraldehyde and then postfixed in 1% OsO_4 in 0.1 M PBS. The slides for scanning electron microscopy images were dehydrated in a graded series of ethanol and dried in the critical point drying apparatus HCP-2 (Hitachi Ltd.) with liquid CO_2. They were spatter-coated with osmium using NL-OPC80N (Filgen) and examined by scanning electron microscope S-4500 (Hitachi Ltd.) and yttrium aluminium garnet (YAG) backscattered detector (Hitachi Ltd.). The slides for transmission electron microscopy observation were dehydrated in a graded series of ethanol and embedded in Epon812. The ultrathin sections were stained with uranyl acetate and then examined with transmission electron microscope H-7100 (Hitachi Ltd.).

Statistics. Individual experiments were performed in at least triplicate. Data are expressed as means ± SEM and were compared using the Mann-Whitney *U* test. A *P* value of less than 0.05 was considered to be statistically significant.

Acknowledgments

The authors thank Peter A. Campochiaro and Sean F. Hackett for the human RPE cells; Tomoko Yoshida for her excellent technical support; Yoshio Miki for gene analysis; and Misaki Sekiguchi and Yukio Matsuda for technical assistance. We also thank Craig Gerard, Harvard Medical School, for providing neprilysin-knockout mice. This work was supported in part by research grants 14657483, 15390558, 16390495, 16390537, 14370555, and 17025046 and the 21st Century COE Program from the Japan Society for the Promotion of Science, Tokyo, Japan.

Received for publication February 2, 2005, and accepted in revised form June 28, 2005.

Address correspondence to: Kyoko Ohno-Matsui, Department of Ophthalmology and Visual Science, Tokyo Medical and Dental University, 1-5-45 Yushima, Bunkyo-ku, Tokyo 113-8519, Japan. Phone: 81-3-5803-5302; Fax: 81-3-3818-7188; E-mail: k.ohno.oph@tmd.ac.jp.

1. Vassar, R., et al. 1999. Beta-secretase cleavage of Alzheimer's amyloid precursor protein by the transmembrane aspartic protease BACE. *Science.* **286**:735–741.
2. Takasugi, N., et al. 2003. The role of presenilin cofactors in the gamma-secretase complex. *Nature.* **422**:438–441.
3. Saido, T.C. 1998. Alzheimer's disease as proteolytic disorders: anabolism and catabolism of beta-amyloid [review]. *Neurobiol. Aging.* **19**:S69–S75.
4. Selkoe, D.J. 2001. Alzheimer's disease: genes, proteins, and therapy [review]. *Physiol. Rev.* **81**:741–766.
5. Iwata, N., et al. 2001. Metabolic regulation of brain Abeta by neprilysin. *Science.* **292**:1550–1552.
6. Iwata, N., Takaki, Y., Fukami, S., Tsubuki, S., and Saido, T.C. 2002. Region-specific reduction of A beta-degrading endopeptidase, neprilysin, in mouse hippocampus upon aging. *J. Neurosci. Res.* **70**:493–500.
7. Hooper, N.M., Karran, E.H., and Turner, A.J. 1997. Membrane protein secretases. *Biochem. J.* **321**:265–279.
8. Wisniewski, T., Ghiso, J., and Frangione, B. 1997. Biology of A beta amyloid in Alzheimer's disease. *Neurobiol. Dis.* **4**:313–328.
9. Maat-Schieman, M.L., van Duinen, S.G., Rozemuller, A.J., Haan, J., and Roos, R.A. 1997. Association of vascular amyloid beta and cells of the mononuclear phagocyte system in hereditary cerebral hemorrhage with amyloidosis (Dutch) and Alzheimer disease. *J. Neuropathol. Exp. Neurol.* **56**:273–284.
10. Uchihara, T., Akiyama, H., Kondo, H., and Ikeda, K. 1997. Activated microglial cells are colocalized with perivascular deposits of amyloid-beta protein in Alzheimer's disease brain. *Stroke.* **28**:1948–1950.
11. Yamada, M., et al. 1996. Immune reactions associated with cerebral amyloid angiopathy. *Stroke.* **27**:1155–1162.
12. Johnson, L.V., et al. 2002. The Alzheimer's A beta -peptide is deposited at sites of complement activation in pathologic deposits associated with aging and age-related macular degeneration. *Proc. Natl. Acad. Sci. U. S. A.* **99**:11830–11835.
13. Dentchev, T., Milam, A.H., Lee, V.M., Trojanowski, J.Q., and Dunaief, J.L. 2003. Amyloid-beta is found in drusen from some age-related macular degeneration retinas, but not in drusen from normal retinas. *Mol. Vis.* **9**:184–190.
14. Anderson, D.H., et al. 2004. Characterization of beta amyloid assemblies in drusen: the deposits associated with aging and age-related macular degeneration. *Exp. Eye Res.* **78**:243–256.
15. Sommer, A., et al. 1991. Racial differences in the cause-specific prevalence of blindness in east Baltimore.

N. Engl. J. Med. **325**:1412–1417.
16. Attebo, K., Mitchell, P., and Smith, W. 1996. Visual acuity and the causes of visual loss in Australia. The Blue Mountains Eye Study. *Ophthalmology.* **103**:357–364.
17. VanNewkirk, M.R., Weih, L., McCarty, C.A., and Taylor, H.R. 2001. Cause-specific prevalence of bilateral visual impairment in Victoria, Australia: the Visual Impairment Project. *Ophthalmology.* **108**:960–967.
18. Oshima, Y., et al. 2001. Prevalence of age related maculopathy in a representative Japanese population: the Hisayama study. *Br. J. Ophthalmol.* **85**:1153–1157.
19. Bird, A.C., et al. 1995. An international classification and grading system for age-related maculopathy and age-related macular degeneration. The International ARM Epidemiological Study Group. *Surv. Ophthalmol.* **39**:367–374.
20. Smiddy, W.E., and Fine, S.L. 1984. Prognosis of patients with bilateral macular drusen. *Ophthalmology.* **91**:271–277.
21. Wang, J.J., Foran, S., Smith, W., and Mitchell, P. 2003. Risk of age-related macular degeneration in eyes with macular drusen or hyperpigmentation: the Blue Mountains Eye Study cohort. *Arch. Ophthalmol.* **121**:658–663.
22. Green, R.G., and Harlan, J.B. 1999. Histopathologic features. In *Age-related macular degeneration*. J.W. Berger, S.L. Fine, and M.G. Maguire, editors. Mosby. St. Louis, Missouri, USA. 81–154.
23. Bressler, S.B., Maguire, M.G., Bressler, N.M., and Fine, S.L. 1990. Relationship of drusen and abnormalities of the retinal pigment epithelium to the prognosis of neovascular macular degeneration. The Macular Photocoagulation Study Group. *Arch. Ophthalmol.* **108**:1442–1447.
24. Hogan, M.J., Alvarado, J.A., and Weddell, J.E. 1971. Retina. In *Histology of the human eye*. W.B. Saunders. Philadelphia, Pennsylvania, USA. 393–522.
25. Marmor, M.F. 1998. Structure, function, and disease of the retinal pigment epithelium. In *The retinal pigment epithelium*. M.F. Marmor and T.J. Wolfensberger, editors. Oxford University Press. New York, New York, USA. 3–12.
26. Kvanta, A., Algvere, P.V., Berglin, L., and Seregard, S. 1996. Subfoveal fibrovascular membranes in age-related macular degeneration express vascular endothelial growth factor. *Invest. Ophthalmol. Vis. Sci.* **37**:1929–1934.
27. Kliffen, M., Sharma, H.S., Mooy, C.M., Kerkvliet, S., and de Jong, P.T. 1997. Increased expression of angiogenic growth factors in age-related maculopathy. *Br. J. Ophthalmol.* **81**:154–162.
28. Okamoto, N., et al. 1997. Transgenic mice with increased expression of vascular endothelial growth factor in the retina: a new model of intraretinal and subretinal neovascularization. *Am. J. Pathol.* **151**:281–291.
29. Schwesinger, C., et al. 2001. Intrachoroidal neovascularization in transgenic mice overexpressing vascular endothelial growth factor in the retinal pigment epithelium. *Am. J. Pathol.* **158**:1161–1172.
30. Folkman, J. 1995. Angiogenesis in cancer, vascular, rheumatoid and other disease. *Nat. Med.* **1**:27–31.
31. Ohno-Matsui, K., et al. 2001. Novel mechanism for age-related macular degeneration: an equilibrium shift between the angiogenesis factors VEGF and PEDF. *J. Cell. Physiol.* **189**:323–333.
32. Tombran-Tink, J., Chader, G.G., and Johnson, L.V. 1991. PEDF: a pigment epithelium-derived factor with potent neuronal differentiative activity. *Exp. Eye Res.* **53**:411–414.
33. Tombran-Tink, J., and Johnson, L.V. 1989. Neuronal differentiation of retinoblastoma cells induced by medium conditioned by human RPE cells. *Invest. Ophthalmol. Vis. Sci.* **30**:1700–1707.
34. Dawson, D.W., et al. 1999. Pigment epithelium-derived factor: a potent inhibitor of angiogenesis. *Science.* **285**:245–248.
35. Stellmach, V., Crawford, S.E., Zhou, W., and Bouck, N. 2001. Prevention of ischemia-induced retinopathy by the natural ocular antiangiogenic agent pigment epithelium-derived factor. *Proc. Natl. Acad. Sci. U. S. A.* **98**:2593–2597.
36. Hardy, J. 1997. Amyloid, the presenilins and Alzheimer's disease. *Trends Neurosci.* **20**:154–159.
37. Shirotani, K., et al. 2001. Neprilysin degrades both amyloid beta peptides 1-40 and 1-42 most rapidly and efficiently among thiorphan- and phosphoramidon-sensitive endopeptidases. *J. Biol. Chem.* **276**:21895–21901.
38. Loffler, K.U., Edward, D.P., and Tso, M.O. 1995. Immunoreactivity against tau, amyloid precursor protein, and β-amyloid in the human retina. *Invest. Ophthalmol. Vis. Sci.* **36**:2–31.
39. Frederikse, P.H., Garland, D., Zigler, J.S., Jr., and Piatigorsky, J. 1996. Oxidative stress increases production of beta-amyloid precursor protein and beta-amyloid (Abeta) in mammalian lenses, and Abeta has toxic effects on lens epithelial cells. *J. Biol. Chem.* **271**:10169–10174.
40. Liang, F.Q., and Godley, B.F. 2003. Oxidative stress-induced mitochondrial DNA damage in human retinal pigment epithelial cells: a possible mechanism for RPE aging and age-related macular degeneration. *Exp. Eye Res.* **76**:397–403.
41. Campochiaro, P.A., and Hackett, S.F. 1993. Corneal endothelial cell matrix promotes expression of differentiated features of retinal pigmented epithelial cells: implication of laminin and basic fibroblast growth factor as active components. *Exp. Eye Res.* **57**:539–547.
42. Saari, J.C., et al. 2001. Visual cycle impairment in cellular retinaldehyde binding protein (CRALBP) knockout mice results in delayed dark adaptation. *Neuron.* **29**:739–748.
43. Curcio, C.A., and Millican, C.L. 1999. Basal linear deposit and large drusen are specific for early age-related maculopathy. *Arch. Ophthalmol.* **117**:329–339.
44. Pereira, C., Ferreiro, E., Cardoso, S.M., and de Oliveira, C.R. 2004. Cell degeneration induced by amyloid-beta peptides: implications for Alzheimer's disease [review]. *J. Mol. Neurosci.* **23**:97–104.
45. Abramov, A.Y., Canevari, L., and Duchen, M.R. 2004. β-amyloid peptides induce mitochondrial dysfunction and oxidative stress in astrocytes and death of neurons through activation of NAPDH oxidase. *J. Neurosci.* **24**:565–575.
46. Butterfield, D.A., and Boyd-Kimball, D. 2004. Amyloid β-peptide(1-42) contributes to the oxidative stress and neurodegeneration found in Alzheimer disease brain. *Brain Pathol.* **14**:426–432.
47. Matsuda, S., Gomi, F., Oshima, Y., Tohyama, M., and Tano, Y. 2005. Vascular endothelial growth factor reduced and connective tissue growth factor induced by triamcinolone in ARPE19 cells under oxidative stress. *Invest. Ophthalmol. Vis. Sci.* **46**:1062–1068.
48. Garg, T.K., and Chang, J.Y. 2003. Oxidative stress causes ERK phosphorylation and cell death in cultured retinal pigment epithelium: prevention of cell death by AG126 and 15-deoxy-delta 12, 14-PGJ2. *BMC Ophthalmol.* **21**:5. doi:10.1186/1471-2415-3-5.
49. Alizadeh, M., Wada, M., Gelfman, C.M., Handa, J.T., and Hjelmeland, L.M. 2001. Downregulation of differentiation specific gene expression by oxidative stress in ARPE-19 cells. *Invest. Ophthalmol. Vis. Sci.* **42**:2706–2713.
50. Fernandez-Robredo, P., Moya, D., Rodriguez, J.A., and Garcia-Layana, A. 2005. Vitamins C and E reduce retinal oxidative stress and nitric oxide metabolites and prevent ultrastructural alterations in porcine hypercholesterolemia. *Invest. Ophthalmol. Vis. Sci.* **46**:1140–1146.
51. Nakagawa, T., et al. 2000. Caspase-12 mediates endoplasmic-reticulum-specific apoptosis and cytotoxicity by amyloid β. *Nature.* **6**:98–103.
52. Holekamp, N.M., Bouck, N., and Volpert, O. 2002. Pigment epithelium-derived factor is deficient in the vitreous of patients with choroidal neovascularization due to age-related macular degeneration. *Am. J. Ophthalmol.* **134**:220–227.
53. Chong, N.H., et al. 2005. Decreased thickness and integrity of the macular elastic layer of Bruch's membrane correspond to the distribution of lesions associated with age-related macular degeneration. *Am. J. Pathol.* **166**:241–251.
54. Klein, R.J., et al. 2005. Complement factor H polymorphism in age-related macular degeneration. *Science.* **308**:385–389.
55. Edwards, A.O., et al. 2005. Complement factor H polymorphism and age-related macular degeneration. *Science.* **308**:421–424.
56. Haines, J.L., et al. 2005. Complement factor H variant increases the risk of age-related macular degeneration. *Science*. **308**:419–421.
57. Cordoba, S.R.D., Esparza-Gordillo, E.G.D., de Jorge, E.G., Lopez-Trascasa, M., and Sanchez-Corral, P. 2004. The human complement factor H: functional roles, genetic variations and disease associations. *Mol. Immunol.* **41**:355–367.
58. Goldstein, L.E., et al. 2003. Cytosolic beta-amyloid deposition and supranuclear cataracts in lenses from people with Alzheimer's disease. *Lancet.* **361**:1258–1265.
59. Meehan, S., et al. 2004. Amyloid fibril formation by lens crystallin proteins and its implications for cataract formation. *J. Biol. Chem.* **279**:3413–3419.
60. Sandilands, A., et al. 2002. Altered aggregation properties of mutant gamma-crystallins cause inherited cataract. *EMBO J.* **21**:6005–6014.
61. Hock, C., et al. 2002. Generation of antibodies specific for β-amyloid by vaccination of patients with Alzheimer disease. *Nat. Med.* **8**:1270–1275.
62. Lombardo, J.A., et al. 2003. Amyloid-beta antibody treatment leads to rapid normalization of plaque-induced neuritic alterations. *J. Neurosci.* **23**:10879–10883.
63. Iwata, N., et al. 2004. Presynaptic localization of neprilysin contributes to efficient clearance of amyloid-beta peptide in mouse brain. *J. Neurosci.* **24**:991–998.